Baghdad Science Journal

Volume 22 | Issue 2 Article 14

2025

Biosynthesis of Silver Nanoparticles by Extracellular Metabolites of Marine Kocuria flava and Investigated Its Role in Enhancing of Antibacterial Activity of Ciprofloxacin

Fadhil Jabbar Farhan
Department of Biology, College of Education for Pure Science, University of Basrah, Basrah, Iraq,
fadhil.farhan@uobasrah.edu.iq

Ali Aboud Shareef
Department of Biology, College of Education for Pure Science, University of Basrah, Basrah, Iraq

Follow this and additional works at: https://bsj.researchcommons.org/home

How to Cite this Article

Farhan, Fadhil Jabbar and Shareef, Ali Aboud (2025) "Biosynthesis of Silver Nanoparticles by Extracellular Metabolites of Marine Kocuria flava and Investigated Its Role in Enhancing of Antibacterial Activity of Ciprofloxacin," *Baghdad Science Journal*: Vol. 22: Iss. 2, Article 14.
DOI: https://doi.org/10.21123/bsj.2024.9965

This Article is brought to you for free and open access by Baghdad Science Journal. It has been accepted for inclusion in Baghdad Science Journal by an authorized editor of Baghdad Science Journal.

BAGHDAD SCIENCE JOURNAL 2025;22(2):507–525

Scan the QR to view
the full-text article on
the journal website

RESEARCH ARTICLE

Biosynthesis of Silver Nanoparticles by Extracellular Metabolites of Marine *Kocuria flava* and Investigated Its Role in Enhancing of Antibacterial Activity of Ciprofloxacin

Fadhil Jabbar Farhan *, **Ali Aboud Shareef**

Department of Biology, College of Education for Pure Science, University of Basrah, Basrah, Iraq

ABSTRACT

The current study aimed to biosynthesize silver nanoparticles (AgNPs) by extracellular metabolites of marine *Kocuria flava*, and characterization it, then use them to enhance the ciprofloxacin activity against MDR pathogenic bacteria. The seawater was collected from the Iraqi Marine Water in January 2022. The isolate *K. flava* (F57) was identified by morphological, some biochemical, and molecular identification by *16S rDNA* amplification and sequencing. The identity (%) of the F57 *16SrDNA* gene with those in GenBank was 99.93%, and the phylogenetic tree showed high identity with *K. flava* strain AUMC B-459. GC/MS spectrometry of the F57 extract revealed the presence of thirty compounds. The extracellular metabolites of F57 are used to biosynthesize of AgNPs., and the production of AgNPs was verified by UV–Vis spectroscopy, FTIR- spectrum, XRD, FESEM, and EDX analysis. The antimicrobial activity of AgNPs was investigated against *Klebsiella pneumoniae*, *Pseudomonas aeruginosa*, *Staphylococcus haemolyticus*, and two isolates of *Escherichia coli* (1&2), the results showed that AgNPs were effective against these pathogens. The minimal inhibitory concentration (MIC) of AgNPs, ciprofloxacin, and their combination was investigated against these MDR pathogens. The lowest MIC of AgNPs. was 7.81 μg/ml against *P. aeruginosa*. All pathogenic bacteria were resistant to ciprofloxacin. The combination of ciprofloxacin and AgNPs had a synergistic effect on *P. aeruginosa, S. haemolyticus,* and *E. coli* (2). The isolates *E. coli* (1&2) became sensitive to ciprofloxacin after being mixed with AgNPs. So, the biosynthesized AgNPs. by extracellular metabolites of marine *K. flava* had antimicrobial properties and contributed to enhancing the effectiveness of ciprofloxacin.

Keywords: AgNPs, Antibiotic enhancement, Ciprofloxacin, *Kocuria flava*, MDR

Introduction

The issue of antibiotic resistance has emerged as a significant concern in recent years due to various factors: among which is the widespread and inappropriate utilization of antibiotics. Therefore, bacteria have developed different strategies of resistance to many antibiotics, rendering them ineffective in combating pathogenic bacteria. Consequently, treating injuries and diseases caused by these pathogens has become increasingly challenging and intricate. Moreover, the risk of disease transmission and the severity of injuries have escalated, making their treatment increasingly difficult and, in some cases, impossible. Consequently, there has been a notable rise in mortality rates associated with these conditions. [1,2]

Nanotechnology is a branch of science and technology that uses materials with tiny dimensions (1–100 nm) in various forms. Since 2004, this technology has advanced, and since 2016, interest in this field has increased. [3] The nanomaterial's composition, structure, and morphology became critical

Received 16 October 2023; revised 2 February 2024; accepted 4 February 2024.
Available online 21 February 2025

* Corresponding author.
E-mail addresses: fadhil.farhan@uobasrah.edu.iq (F. J. Farhan), aliaboud547@gmail.com (A. A. Shareef).

https://doi.org/10.21123/bsj.2024.9965
2411-7986/© 2025 The Author(s). Published by College of Science for Women, University of Baghdad. This is an open-access article distributed under the terms of the Creative Commons Attribution 4.0 International License, which permits unrestricted use, distribution, and reproduction in any medium, provided the original work is properly cited.

due to the advancement of nanoparticle characterization technologies and growing interest. On the other hand, since it can directly kill both Gram-positive and Gram-negative pathogenic bacteria and it acts as a delivery of other antibacterial agents that make them overcome multidrug resistance (MDR) bacteria because they can attack and affect the bacterial cell by targeting several scorings in bacterial cells frequently cannot resist them, it could be a promising solution to replace antibiotics to overcome bacterial resistance. By degrading the peptidoglycan without penetrating the cell, the nanomaterials can target the bacterial cell wall and prevent the formation it, causing the production of free radicals like hydrogen peroxide, which causes oxidative stress within the cell and, ultimately, cell death by preventing or altering the production of essential proteins required for growth, replication, crucial metabolic processes, and enzymatic activity within the cell, it can cause a hole to form in the plasma membrane, rendering it useless, and it can also impact DNA and RNA by preventing the production of nitrogenous bases necessary for synthesizing these nucleic acids, thereby resulting in preventing replication, and effect on biofilms by covering the entire surface and acting as a barrier between it and the outside environment and closing exchange channels between it and the environment, this makes the majority of the mechanisms used by pathogenic bacteria for antibiotic resistance useless, thus reducing the likelihood of infection.[4]

Among other metallic nanomaterials, silver nanoparticles (AgNPs) are of particular interest because of their numerous uses in nanomedicine, the manufacturing of sports shoes, cosmetics, wound dressings, their antibacterial and anticancer properties. It may be utilized for medication delivery and molecular sensing.[5] Li et al.[6] pioneered investigating the potential synergy of silver nanoparticles and amoxicillin in combating *E. coli*, they observed that when silver nanoparticles were employed with this antibiotic, it significantly reduced the minimum inhibitory concentration (MIC) values. Singh et al.[7] found a noticeable synergistic action of silver nanoparticles synthesized utilizing the bacterium *Acinetobacter calcoaceticus*, This was achieved by enhancing the efficacy of various antibiotics; among these antibiotics is ciprofloxacin that exhibits efficacy against pathogenic bacteria, particularly against Gram-negative strains. Tharwat et al.[8] employed a combination of silver nanoparticles with ciprofloxacin to combat the antibiotic-resistant pathogenic bacteria Pseudomonas aeruginosa. The utilization of nanoparticles has shown a notable synergistic impact in augmenting the efficacy of the antibiotic and impeding the proliferation of bacteria. The study conducted by Khalil et al.[9–11] involved the examination of the potential synergistic effects between silver nanoparticles produced by the marine actinobacteria *Nocardiopsis dassonvillei* and *Streptomyces catenulae*, and several antibiotics, among them is ciprofloxacin. Utilizing these nanomaterials results in a synergistic impact on reducing MIC values against pathogenic *Pseudomonas aeruginosa*. In a study conducted by Haji et al.[12] they were observed that the utilization of *Acinetobacter baumannii* in the preparation of silver nanoparticles resulted in a noteworthy synergistic impact, leading to enhanced efficacy of several antibiotics, among them was ciprofloxacin, and has been found to effectively decrease the MIC values of this antibiotic against multidrug resistance bacteria. Consequently, the application of these nanoparticles in nanomedicine has been suggested.

The nanoparticles produced by microorganisms have a significant level of stability. They are evenly distributed, which increases their effectiveness because the substances used in the silver nitrate reduction process (the raw material that is converted into silver nanoparticles by the enzymatic action of bacteria) encapsulate these particles, prevent their accumulation, and aggregate them with one another without the need for other capping materials. This process is secure, eco-friendly, quick, affordable, and does not use energy because it does not use heat.[13]

The emergence of antibiotic resistance among pathogenic bacteria and its consequential implications on public health and the global economy have prompted researchers to explore alternative approaches to combat this issue. One way of investigation involves the utilization of nanoparticles to enhance the efficacy of existing antibiotics or to identify potential alternatives. The subject under discussion is the utilization of nanoparticles in drug and antibiotic delivery systems, specifically the Nanoparticulate Antibiotic-Delivery System (DDS). This innovative approach enables the design of nanocarriers that effectively transport pharmaceutical drugs and antibiotics to pathogenic bacteria cells or cancer cells.[9] So, the current study was conducted to biosynthesize and characterize AgNPs. by extracellular metabolites of marine *K. flava*, and the role of these nanoparticles in enhancement of the effectiveness of ciprofloxacin against pathogenic bacteria that are resistant to it.

Materials and methods

Sample collection and bacterial cultivation

Seawater samples were obtained from the Shatt Al-Arab River Estuary, North-West Arabian Gulf, at the Iraqi Marine Water region. The Global Positioning

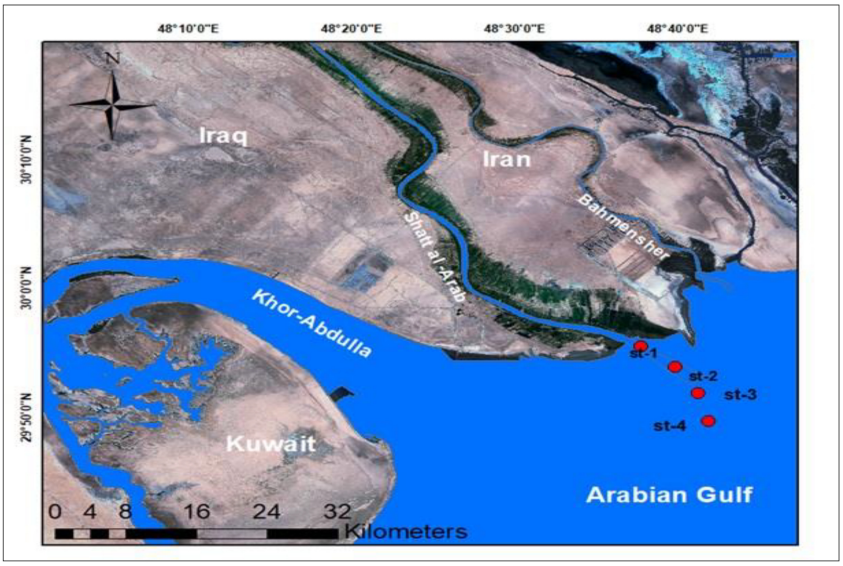


Fig. 1. Sampling stations for the collection of marine water samples within Iraqi marine waters.

System (GPS) determined the various locations (St.1: 29.90"209" North- 48.64"88" East. St. 2: 29.85"12" North- 48.71"71" East. St. 3: 29.90"20" North- 48.75"63" East. and St. 4: 29.77"65" North- 48.76"86" East) Fig. 1. The collection was conducted in January 2022 using a water sampler (Wildco, USA). The samples were taken at a depth of 10–15 cm and stored in sterile glass containers with a capacity of 500 ml. Containers were stored in an ice box and transferred to the Microbiology laboratory for postgraduate studies, Department of Biology, College of Education for Pure Science, University of Basrah. During the collecting procedure, many environmental parameters were measured, such as temperature, pH, conductivity (EC), salinity, total dissolved salts (TDS), and percentage of dissolved oxygen (DO%) by using a multimeter (HORIPA, Japan).[11]

A serial dilution was made using a sterile normal saline solution (85% NaCl). Subsequently, they were cultured on Zobell marine agar 2216 plates (HiMedia, India), and the final pH of the medium was adjusted to 7.5 ± 0.2. The plates were incubated at 25 ± 2°C for 5–7 days.[14] Following the incubation period, the bacterial isolates were subsequently sub-cultured on a nutrient agar medium to get pure colonies.[15]

Morphological and microscopic characteristics

The morphological attributes of the bacterial isolate colonies on agar plates were observed using a dissecting microscope to characterize their form, margin, texture, and pigmentation. The utilization of 3% KOH and Gram stain (HiMedia, India) was employed to differentiate between Gram-positive and Grame-negative bacteria. The light microscope was employed to observe the morphology of cells, including their various shapes such as cocci, bacilli, or others. The use of 3% hydrogen peroxide was employed for the assessment of the isolate's capability to produce catalase. The catalase test was employed to differentiate between aerobic and anaerobic microorganisms.[16]

DNA extraction and purification

The genomic DNA (gDNA) of bacterial isolates was extracted using the Presto ™ Mini gDNA bacteria kit (Geneaid, Taiwan), based on the worksheet included in the kit. Following the extraction and purification process of bacterial DNA, it was confirmed using electrophoresis utilizing a 1% agarose gel (Bioneer, Korea) submerged in Tris-Borate-EDTA (TBE) solution. To see the DNA, ethidium bromide (Promega, USA) was employed as a staining agent. The DNA solution was kept at a temperature of –20°C.

16S rDNA gene amplification and nucleotide sequencing

To amplify the *16S rDNA* gene, the Polymerase Chain Reaction (PCR) technique was employed utilizing a universal primer set. The forward primer used was 27F (5′- AGAGTTTGATCCTGGCTCAG-3′), whereas the reverse primer used was 1492R (5′-GGTTACCTTGTTACGACTT-3′).[17] The PCR mixture consisted of 25 μl of master mix (Promega, USA), 2 μL from each of the forward and reverse primers, 5 μL of gDNA, and 16 μL of nuclease-free water (Bioneer,

Korea). The total volume of the mixture was 50 μL, which was prepared in a 200 μL PCR tube. The PCR tubes were positioned into the Thermocycler device (DLAB, USA). The amplification protocol consists of the following steps: an initial denaturation at 94°C for 5 minutes, followed by 35 cycles of denaturation at 94°C for 30 seconds, primer annealing at 55.5°C for 30 seconds, and extension at 72°C for 90 seconds. Finally, there is one cycle of final extension at 72°C for 5 minutes.[18] The verification of the PCR products was conducted by electrophoresis using a 2% agarose gel in TBE buffer. Ethidium bromide was employed as a staining agent for the amplified gene. The PCR products (1550 bps) were subsequently sent to Macrogen, Seoul, South Korea, to ascertain the nucleotide sequence of the *16SrDNA* gene. The *16SrDNA* gene sequence that was acquired was subjected to comparison with the reference sequence available in the NCBI GeneBank database, utilizing the BLAST algorithm. The molecular Evolutionary Genetic Analysis (MEGA 11) program is used to construct a phylogenetic tree employing the maximum likelihood algorithm.[19]

Preparation of extracellular bacterial extracts

The cell-free extract was obtained by cultivating a pure bacterial isolate on nutrient agar plates (HiMedia, India) at 28 ± 2°C for 4–5 days. Luria-Bertani broth (LB) medium (HiMedia, India) was prepared in a 1000 mL conical flask and sterilized using an autoclave. The sterile LB medium was inoculated with a freshly bacterial isolate. Then, the flask containing the inoculated medium was placed in a shaker incubator (LabTech, Korea) and incubated at a temperature of 37 ± 2°C, with continuous shaking at a speed of 180 rpm for 4–5 days. Following the incubation phase, the bacterial growth underwent centrifugation at 8000 rpm for 10 minutes. The resulting supernatant was subsequently utilized in the process of biosynthesizing silver nanoparticles.[15]

Determination of active chemical compounds in the extracellular bacterial supernatant

The identification of the active chemical compounds that might engage in the reduction of silver ions to silver nanoparticles in the extracellular extract of bacterial supernatant was achieved through the utilization of Gas chromatography-mass spectrography (GC-MS) (Agilent, USA). The methodology employed in this study followed the procedure outlined by Naveed et al.[20] The extracellular bacterial supernatant was subjected to extraction using the organic solvent Ethyl acetate, followed by concentration through evaporation at a temperature of 55°C. This process resulted in the production of a red-colored crude extract. The active biomolecules were identified by introducing 2 μL of the unrefined extract into the instrument employing an Elite5MS column. The model's source and transfer temperatures were established at 150°C, and scanning was conducted throughout a mass range of 50–600.

Biogenic synthesis of silver nanoparticles

The biosynthesis of silver nanoparticles was conducted using an extracellular extract of a bacterial isolate (supernatant), as outlined in the study by Huq and Akter.[15] Briefly, a volume of 100 mL of supernatant was transferred into a sterile conical flask with a capacity of 250 mL and thereafter shielded from light exposure using aluminum foil. A total of 0.0169 grams of $AgNO_3$ (Alfa, India) was introduced into the flask, resulting in a final concentration of $AgNO_3$ of 1 mM. The mixture was placed in the shaker incubator, where it was subjected to a temperature of 37 ± 2°C and an agitation speed of 180 rpm for 5–7 days. The initial indication of biosynthesized silver nanoparticles was observed by the transition of the mixture color, shifting from yellow to dark brown.

Characterization of biosynthesized silver nanoparticles

UV-Visible spectroscopy

The spectrum of UV-visible radiation was determined in the Dept. of Biology, College of Education for Pure Sciences, University of Basrah, to ensure the formation of silver nanoparticles by examining their optical properties. The dilute solution of silver nanoparticles was prepared using deionized distilled water (DDW). The absorbance was measured using a UV-Visible spectrophotometer (Aquarius, England) and a quartz cuvette at a wavelength between 280–800 nm and observing the formant and a plasmon spectrum indicating the reduction of silver ions to silver nanoparticles.[21]

Fourier transform infrared spectroscopy (FTIR)

An infrared spectrum test was conducted in the Dept. of Chemistry, College of Education for Pure Sciences, University of Basrah, to determine the active groups in the bacterial extract that act as reducing silver ions to silver nanoparticles (AgNPs). Samples were prepared by drying each of the bacterial extracts and the resulting silver nanoparticles in an electric oven (Binder, Germany) at a temperature of 40°C; the dry samples were mixed with potassium bromide (KBr) and it was packed in a small press. The powder

was pressed to obtain a very thin transparent pellet. It was examined with a Fourier transform infrared (FTIR) spectrometer at room temperature and within a range of 400–4000 cm^{-1} an accuracy level of 4 cm^{-1}. The spectrum was compared with the reference tables to know the active groups. [21]

X-ray diffraction (XRD)

X-ray diffraction (XRD) analysis was carried out with an X-ray diffractometer in the Islamic Republic of Iran to determine the crystalline nature of silver nanoparticles. A silver nanoparticle powder was prepared in an electric oven at 40°C, and the dry sample used in an X-ray diffraction pattern was examined using a copper electrode. [21]

Determination of size and shape of silver nanoparticles

The morphological and structural characterization of the biosynthesized silver nanoparticles in the Islamic Republic of Iran was conducted, where the silver nanoparticles were sent to determine the morphological characteristics (size and shape) of the nanoparticles using a scanning electron microscope (SEM), as well as knowing the elemental composition in the particles by measuring the Energy Dispersive of X-ray spectroscopy (EDX) attached to the same scanning electron microscope. [21]

Antimicrobial activity of biosynthesized silver nanoparticles

Five pathogenic bacterial isolates *K. pneumoniae*, *P. aeruginosa*, *S. haemolyticus*, and two isolates of *E. coli* (1&2) were obtained from Al-Fayhaa Teaching Hospital in the Government of Basrah. Isolates were transferred to the microbiology laboratory for postgraduate studies in the Dept. of Biology, College of Education for Pure Sciences, University of Basrah in nutrient agar plane tubes. Then, they were grown on nutrient agar plates by the streaking method.

A dilution of 1000 μg/ml of silver nanoparticles was prepared by dissolving 0.01 g in 1 ml of Dimethyl sulfoxide solvent (DMSO) and supplementing the volume to 10 ml with sterile DDW in a sterile test tube, then the suspension was dissolved by sonicating using an ultrasonic water bath (Fuyang, China) at a temperature of 35°C for 10 minutes. A serial of dilutions was done from the stock dilution using DDW to get several concentrations of 500, 250, and 125 μg/ml. These dilutions were stored in a refrigerator, shielded from light, until they were used. Sterile Muller Hinton agar (MHA) (HiMedia, India) plates were prepared. The bacterial suspension was made by carrying a loopful from the fresh-pure bacterial culture and immersing it in 10 ml of sterile 0.85% normal saline solution. The concentration of the bacterial suspension was adjusted to 0.5 McFarland ($1.5*10^8$ CFU). [16]

The antibacterial efficacy of biosynthesized silver nanoparticles was evaluated against pathogenic bacteria using the agar-well diffusion method, as modified by Perez et al. [22] The bacterial suspension was evenly distributed over the MHA plate surface using a sterile cotton swab. The dishes were set aside for 10 minutes to facilitate the drying of the suspension. In this experiment, a total of four wells were created in each plate using an agar sterile stainless-steel borer that had a 6 mm diameter. About 85 microliters of each dilution from a serial dilution of silver nanoparticles were carefully dispensed into each well using a micropipette. The negative control involved adding 85 microliters of DMSO solvent and DDW to the wells in each plate containing the suspension of pathogenic bacteria being investigated. The plates were incubated at 37°C for 24 hours. Then, the diameters of the inhibition zones of bacterial growth were measured with a measuring scale, serving as indicators of the biological activity of the silver nanoparticles, and were assessed. The experiment was conducted in triplicate to ensure its validity and reliability.

Synergism of biosynthesized silver nanoparticles with ciprofloxacin by micro-dilution method

The investigation involved the evaluation of the combined effects of silver nanoparticles in combination with ciprofloxacin antibiotic using the microtiter dilution method (checkerboard method), as described by Bellio et al. [23] and Khalil et al. [10] Serial dilutions (62.50, 31.25, 15.62, 7.81, 3.90, and 1.95 μg/ml) were prepared from silver nanoparticles stock solution by using Mueller-Hinton broth in sterile test tubes and stored under refrigeration until they were employed. Subsequently, Serial dilutions were conducted using a stock solution of ciprofloxacin antibiotic with a concentration of 1000 μg/ml. The dilutions were generated in tubes, resulting in concentrations of 128, 64, 32, 16, 8, 4, 2, 1, 0.5, and 0.25 μg/ml, and stored in a refrigerator at 4°C.

The 200 μL of each dilution of the silver nanoparticles was added to column B2–G7 of microtiter plates (96 wells). Then, 100 μL from a concentration of 62.5 μg/ml of silver nanoparticles was introduced into the well of row B2–B11 in the microtiter plate. This process was repeated for concentrations in row C2–C11, with the final concentration of 1.95 μg/ml in row H2–H11. The 200 μL of each dilution of the ciprofloxacin was added to row A2–A11 of

microtiter plates. Then, 100 μL from a concentration of 128 μg/ml of this antibiotic was introduced into the well of column A2-G2 in the microtiter plate. This process was repeated for concentrations in column A3–G3, with the final concentration of 0.25 μg/ml in column A11–G11. A volume of 20 μL of 0.5 McFarland bacterial suspension was introduced into the wells of a plate that contained dilutions of silver nanoparticles, as well as the antibiotic ciprofloxacin. Furthermore, the wells also included a combination of the nanoparticles with the antibiotic. A volume of 200 μL of MHB was introduced into the wells of column A12–H12, and then 20 μL bacterial suspension was added to this column as the positive control. As a negative control, the serial concentrations of silver nanoparticles and ciprofloxacin were added into wells of another microtiter plate as above. A volume of 200 μL of MHB was added into the wells of column A12–H12, and no bacterial suspension was given to this plate.

The optical density (OD) of each plate was measured using an ELISA plate reader (Thermo-Fisher Scientific, USA) at a wavelength of 620 nm before and after incubation at a temperature of 37°C for 24 hours; ten measurements were taken for each well. The MIC* was assessed by the observation of turbidity, along with the use of the following equation: [24]

Growth Inhibition (GI%) = 100 – (OD of drug ÷ OD of control)*100
***The MIC values are the lowest antimicrobial agent that inhibit more than 80% of bacterial growth** [23]

To determine the correlation between silver nanoparticles and ciprofloxacin, the Fractional Inhibitory Concentration Index (FICI) was calculated by an equation described by Fadwa et al. [25] as follows:

$$\mathbf{FICI = FIC_{Ab.} + FIC_{NPs.}}$$

Where: $FIC_{AB.}$ Fractional Inhibitory Concentration of the antibiotic, $FIC_{NP.}$ is the Fractional Inhibitory Concentration of silver nanoparticles. It was calculated by the following equation:

$$\mathbf{FIC_{Ab.}} = \text{(MIC of Ab. In the presence of NP.)/(MIC of Ab. alone)}$$
$$\mathbf{FIC_{NP.}} = \text{(MIC of NP. In the presence of Ab.)/(MIC of NP. alone)}$$

The effect was considered synergistic, that is, there is a interaction and combined effect between silver nanoparticles and the antibiotic, resulting in an increase in the antibacterial activity of both substances against pathogenic bacteria, when the FICI $\leq$ 0.5, the effect was deemed partial synergy, when 0.5 $<$ FICI $<$ 1, the effect was deemed additive (silver nanoparticles enhance the efficacy of antibiotics against pathogenic bacteria), when FICI = 1. Conversely, when no interaction between the silver nanoparticles and the antibiotic, and the total effects are equal to the individual effect of each of them (indifference) when the 1 < FICI < 4. However, when the FICI > 4, an antagonistic effect is observed, i.e., there is a conflict in action between silver nanoparticles and antibiotics, which leads to a reduction of the effectiveness of each of them against pathogenic bacteria. [24]

Statistical analysis

SPSS version 23 was used to investigate the biological efficiency of biosynthesized silver particles against pathogenic bacterial isolates. The study used multivariate analysis of variance with a least significant difference test in the dimensional test by using the Last Significant Difference (LSD) to compare averages under probabilities $\leq$0.05.

Results and discussion

The environmental factors measurement of sampling stations

The environmental measurements conducted in the sampling stations revealed that these locations fall within the marine environment. This determination is based on the high levels of salinity observed, accompanied by moderate acidity and a tendency towards slight alkalinity, which can be attributed to the presence of elevated concentrations of salt ions. The sample collection period exhibited low temperatures and a low concentration of total dissolved salts (TDS), as shown in Table 1.

The above environmental parameters were chosen because they affect microbial diversity and density. Temperature is the main indicator of water quality and aquatic life, it effects the concentration of dissolved oxygen in water. [26] The investigation found that the reported values fell within the yearly average of 10–21°C for the study sites. The concentration of the DO varied between 2.01 and 3.37 mg/l. The water waves facilitate the dissolution of oxygen in water. The process of photosynthesis carried out by algae and aquatic plants contributes to the provision of dissolved oxygen in aquatic environments. [27] D.O. has a significant role in influencing the levels of aquatic biodiversity. All living organisms, including bacteria, particularly those that thrive in aerobic conditions, require oxygen as a final electron acceptor.

The salinity levels exhibited variable values, with a measurement of 27.4 ppt seen in the St. 1, while the St. 3 recorded a higher salinity level of 44.1 ppt.

Table 1. The environmental factors measurement of sampling stations.

Sampling station	Temp. (°C)	DO (mg/L.)	Salinity (ppt)	pH	TDS (g/L.)
St. 1	13.0	2.01	27.40	8.0	26.4
St. 2	13.6	2.58	37.90	8.0	34.7
St. 3	14.7	2.11	44.10	8.2	39.5
St. 4	14.9	3.37	43.96	8.3	35.5

The salinity of water, particularly sodium chloride salt and other dissolved salts, is a significant factor in determining the ecological conditions for aquatic organisms, different bacterial species exhibit varying levels of tolerance to salinity.[27] The pH values indicate that the Iraqi marine water tends to be slightly alkaline. This can be attributed to the presence of calcium and sodium salts within these waters. The pH values have an impact on the microbial diversity within the marine environment. The solubility of many compounds in water, including ammonia, chloride, and mineral elements, may be effected by many factors that tend to alter acidity levels.[27]

The presence of elevated salinity and total dissolved salts, reduced levels of dissolved oxygen and temperatures, as well as pH values, are indicative of the harsh and extreme environmental conditions observed in the Iraqi marine water (places where the samples were collected). These characteristics are reflected in the richness of bacterial species found in the samples. This ecological niche necessitates the presence of halophilic bacteria capable of withstanding elevated levels of total dissolved salts and low temperatures. The environmental factors identified in this study exhibit similarities to those established by Jaafar et al.[28]

Phenotypic and biochemical identification of bacteria

Several bacterial isolates obtained from the Iraqi marine water were subjected to phenotypic and microscopic analysis, as well as some biochemical tests. The results indicated that these isolates were aerobic and Gram- positive bacteria that were tested by Gram stain, and 3% KOH solution and exhibited catalase. Two isolates of actinomycetes were observed exhibited a modest growth rate, requiring an incubation period of approximately 5–7 days. One of these isolates had the characteristic of generating colonies that resembled soft, white cotton mycelia on the nutrient agar medium. Additionally, these isolates displayed the presence of aerial hyphae during growth. The colonies display a robust adhesion to its surface, and they could secrete a pigmented substance, imparting a dark brown hue to the medium. The cells were observed to possess an extended morphology and were organized in the configuration of elongated, branched chains. The isolates were taxonomically identified as members of the genus *Streptomyces* sp. The second isolate has colonies exhibiting a yellow hue during cultivation on nutrient agar. When observed under the light microscope, the cells exhibited a diminutive size and a spherical shape. The cells were arranged in pairs or chains of varying lengths with no endospore forming, and were taxonomically recognized as members of the genus *Kocuria* sp. which was given the F57 symbol.

The presence of Gram-positive bacteria in the study areas is due to their ability to adapt to the harsh marine ecological conditions. These bacteria can tolerate high hydrostatic pressure in sea water, which can damage enzymes and proteins. This was achieved through gene expression changes and increased unsaturated fatty acids in cell membranes increase compactness and plasma membrane stiffness.[29] Additionally, this organism's cell wall has numerous layers of peptidoglycan and teichoic acid, this composition improves cell stiffness, allowing them to endure hydrostatic pressure from the water column. Moreover, most Gram-positive bacteria exhibit a diverse range of temperature tolerance and varying degrees of pH and salinity, owing to their ability to produce extracellular enzymes such as protease, amylase, and cellulase, as well as some possessing the capability to form endospores. The outside surface of the spore also serves as a location for the enzymatic activity involved in oxidation and reduction reactions, which aids in the defense against the harmful effects of various elements and heavy compounds that frequently encounter the endospores.

Syakti et al.[14] found similar results, collecting 51 bacterial isolates from Pacific Ocean waters in Indonesia, all isolates were Gram-positive. Goel et al.[21] and Khalil et al.[10,11] conducted studies on the isolation of actinobacteria from sediments and marine waters. These bacteria were found to thrive in neutral to basic waters with a pH range of 7.0–9.0. Additionally, they exhibited the ability to produce secondary metabolites across a broad temperature range of 10–40°C. This facilitates the elimination of competition and the mitigation or removal of the toxicity associated with diverse heavy chemicals and elements.

Table 2. The *16SrDNA* sequence of F57 and identity% with reference strain.

Query	Nc	Reference	Identity%	Gaps%	Query cover
F57 *16SrDNA* gene	1382	ON843620.1 *Kocuria flava* strain AUMC B-459	1381/1382 99.93%	(0/1382) 0%	100%

Genotypic identification of bacteria by 16S rDNA

A molecular diagnostic approach was employed to analyze bacterial isolates derived from Iraqi marine waters and pathogenic strains, to verify the identification of the isolates at the species level. Distinct DNA bands were acquired through electrophoresis on 1% agarose. F57 isolate was obtained when the universal primers 27F and 1492R were utilized in the PCR to amplify the *16SrDNA* gene. This was evident from the presence of distinct bands with a size of 1500 bps. according to Lader on the conducting electrophoresis on a 2% agarose. The results of alignment of the nucleotide sequences of the *16SrDNA* gene of isolate F57 with the reference sequences of bacterial strains archived in the NCBI GenBank, utilizing the BLAST tool, indicated that it indicated a high degree of identity (99.93%) with the *Kocuria flava* strain AUMC B-459 Table 2. The phylogenetic tree for the F57 isolate, which was constructed by using the Maximum Likelihood algorithm, with Bootstrap analysis was performed for 1000 replications in the MEGAII program. The bootstrap value over was 95% at the nodes of the evolutionary tree branches. F57 isolate was found among a subgroup consisting of various species and strains belonging to the genus *Kocuria*. It was observed to form a distinct cluster alongside the *Kocuria flava* strain AUMC B-459 Fig. 2.

Zhou et al.[30] isolated *K. flava* from the atmospheric environment of Xinjiang, China. They subsequently designated this strain as a reference specimen in the NCBI GenBank. Additionally, they mentioned that the bacteria thrive within a pH range of 7.0–9.0, which is considered neutral to alkaline. Moreover, they exhibit a remarkable tolerance towards elevated levels of sodium chloride salt, surpassing 100 ppt. This unique adaptation enables these bacteria to flourish and proliferate in the Iraqi marine water. Members of this species has the capacity to produce several enzymes, such as protease, lipase, amylase, urease, phosphatase, gelatinase, and β-glucuronidase,[30] these enzymes facilitating their

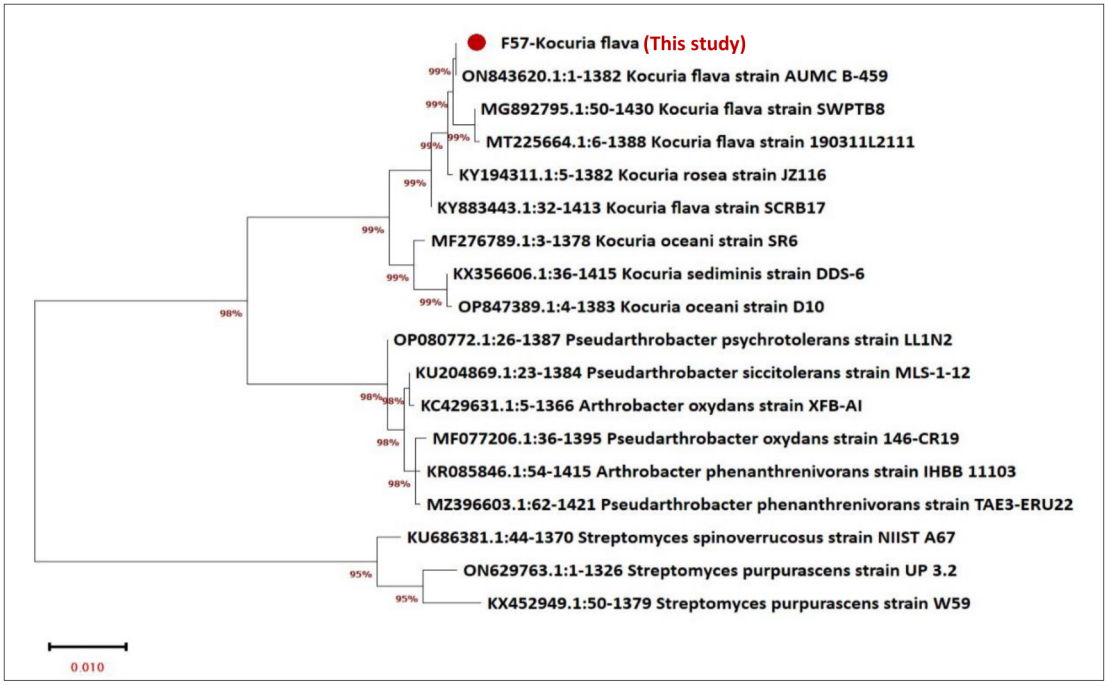


Fig. 2. The construction of a phylogenetic tree depicting the relationship between *K. flava* F57 and other reference strains. The bootstrap analysis consists of 1000 replicates that serve as representative samples of the evolutionary history of the taxa. The scale bar represents a value of 0.10 substitutions per nucleotide location.

Table 3. Chemical compounds found in *Kocuria flava* culture supernatant using GC/MS spectroscopy.

Peak NO.	Compound name	Area%	RT%
1.	Thiodiglycol	0.6777	9.976
2.	2-Pyrrolidinone	2.7580	11.475
3.	3-Methyl-2-pyrrolidinone	0.4503	12.233
4.	Succinic acid, ethyl 2-methylpent-3-yl ester	0.7070	12.956
5.	D-Alloisoleucine	0.3122	16.828
6.	2,5-Piperazinedione, 3-methyl-6-(1-methylethyl)-	0.8841	19.228
7.	2(1H)-Quinolinone, 3,4-dimethyl-	0.2957	19.665
8.	3-Methyl-2,3,6,7,8,8a-hexahydropyrrolo[1,2-a] pyrazine-1,4-dione	5.8584	20.004
9.	3-Methyl-2,3,6,7,8,8a-hexahydropyrrolo[1,2-a] pyrazine-1,4-dione	2.6884	20.245
10.	Pyrrolo [1,2-a] pyrazine-1,4-dione, hexahydro-	29.1357	20.700
11.	Propyl S-2-diisopropylaminoethyl ethylphosphonothiolate	0.9455	20.816
12.	Cyclo(L-prolyl-L-valine)	2.3934	21.137
13.	Cyclo(L-prolyl-L-valine)	1.7149	21.387
14.	Hexahydro-3-(1-methyl propyl) pyrrolo[1,2-a] pyrazine-1,4-dione	1.5410	22.092
15.	Pyrrolo[1,2-a] pyrazine-1,4-dione, hexahydro-3-(2-methylpropyl)-	3.8231	22.270
16.	2,5-Cyclohexadiene-1,4-dione, 2,5-dihydroxy-3-methoxy-6-methyl	7.7097	22.877
17.	2-(Dimethylamino)-3-methyl-1-butene	2.0771	23.100
18.	2H-Azepin-2-one, hexahydro-4-methyl-	2.4315	23.412
19.	9-Vinylcarbazole	1.0873	23.849
20.	2,5-Piperazinedione, 3-methyl-6-(phenylmethyl)-	0.3641	24.063
21.	1,2-Benzenediamine	1.3353	24.340
22.	2,5-Piperazinedione, 3,6-bis(2-methylpropyl)-	20.7496	24.670
23.	Hexahydro-3-(1-methyl propyl) pyrrolo[1,2-a]pyrazine-1,4-dione	0.5802	25.081
24.	2,5-Piperazinedione, 3-benzyl-6-isopropyl-	0.4325	25.313
25.	Pyrrolo[1,2-a] pyrazine-1,4-dione, hexahydro-3-(phenylmethyl)-	0.8185	25.937
26.	Pyrrolo[1,2-a] pyrazine-1,4-dione, hexahydro-3-(phenylmethyl)-	1.4804	26.294
27.	Isovaleramide, N-(2-butyl)-N-nonyl-	0.3022	27.168
28.	7-Hydroxycoumarin	2.2591	27.552
29.	2-Fluorobenzoic acid, 6-chlorohexyl ester	1.4750	27.900
30.	trans-1,4-Cyclohexanedicarbohydrazide	2.3221	28.239

utilization of multiple sources of energy, and they aid in their resistance against the deleterious impacts of organic contaminants and heavy metals, hence facilitating detoxification. Sun et al.[31] isolate *K. flava* from the South China Sea. Upon analysis, they discovered that the genome of the marine isolate S43 was 3,548,480 bp. Notably, this genome was determined to be larger than the genome of strain HO-9041, which was obtained from an air sample and had an evolutionary relationship with S43 as depicted in the constructed phylogenetic tree. The nucleotide pair count of 3,504,335 was observed, which corresponded to the number of genes encoding functional proteins. Specifically, the S43 isolate contained 3,194 genes, while the HO-9041 isolate contained 3,113 genes. Additionally, the marine isolate exhibited a higher number of operon copies, with four copies compared to the three copies found in the other strain. So, the marine isolate exhibited a greater abundance and diversity of proteins, indicating its advantageous adaptation to the challenging marine environment through mechanisms like as osmoregulation and resistance to the detrimental impacts of heavy chemicals and elements.

Determination of active chemical compounds in the extracellular bacterial supernatant

The results of spectroscopic analysis of the bacterial culture supernatant using GC/MS spectrometry revealed the presence of thirty compounds with varying concentrations. Among these compounds, the highest concentration was observed for Pyrrolo [1,2-a] pyrazine-1,4-dione, hexahydro- (Area% = 29.7). This was followed by 2,5-Piperazinedione, 3,6-bis (2-methylpropyl)- (Area% = 20.7496), and then Cyclohexadiene-1,4-dione, 2,5-dihydroxy-3-methoxy-6-methyl- (Area% = 7.7097) Table 3, Fig. 3.

Gas chromatography–mass spectrometry (GC/MS) technique has been used to identify the active compounds in bacterial extract by many researchers to identify compounds that can reduce silver ions into silver nanoparticles and capping them. Deutsch et al.[32] used this technique, and they found many organic compounds such as alcoholic and phenolic compounds, amino acids, ketones, and esters in various concentrations in *Kocuria* flava extract that isolated from Mediterranean Sea marine algae leaves.

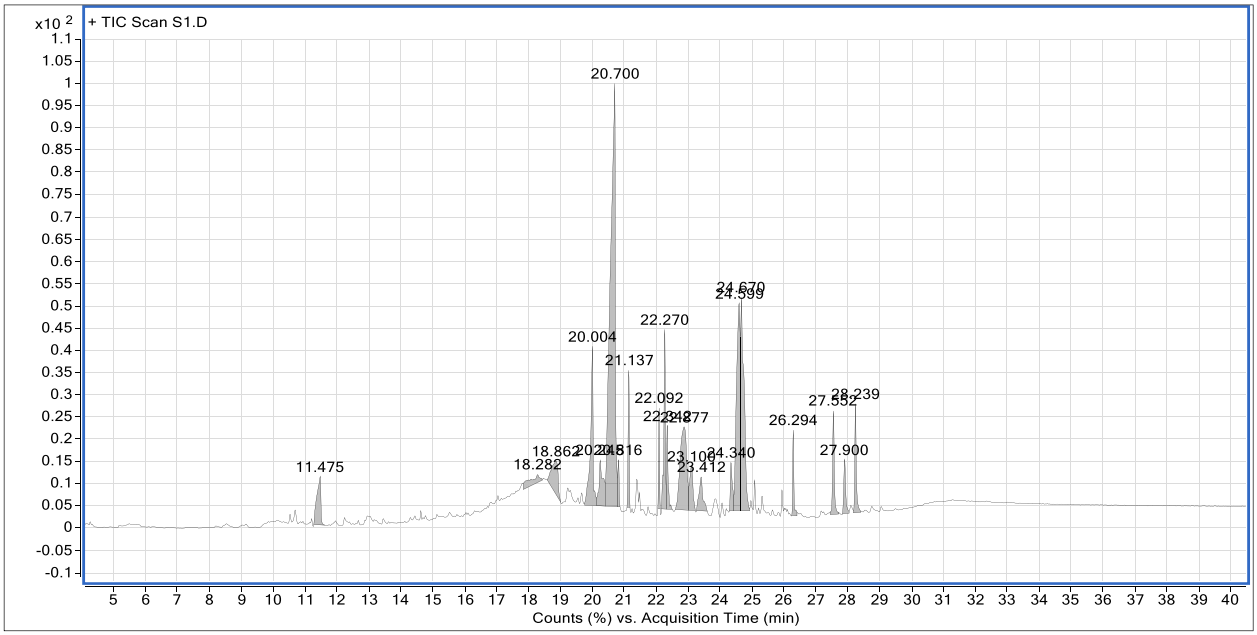


Fig. 3. The GC/MS spectroscopy of *K. flava* culture supernatant.

The pyrrolo[1,2-a] pyrazine-1,4-dione, hexahydro- is a secondary metabolite comes from microorganisms. Kiran et al.[33] extracted this compound from *Bacillus tequilensis* which isolated from sea sponges, this substance had biological activity against MDR *Staphylococcus aureus*, non-toxic to normal cells and had antioxidant activity because it can be scavenging free radicals. This agrees with Ser et al.,[34] who identified this chemical in *Streptomyces* sp. Other studies had indicated its effectiveness against fungi, viruses, parasites, algae, and anticancer activity.[35,36] At peak 8 and 9, 3-Methyl-2,3,6,7,8,8a-hexahydropyrrolo[1,2-a] pyrazine-1,4-dione had methyl groups. This chemical was found at 5.8584% and 2.6884%. Manimaran and Kannabiran[37] found this chemical in *Streptomyces* sp. They demonstrated its antioxidant and free radical-scavenging properties.

Moreover, natural products 2,5-Piperazinedione, 3,6-bis (2-methyl propyl) had therapeutic properties. Several studies have shown it had antimicrobial and antifungal properties, and as an electron acceptor. It found in *Lactobacillus plantarum* and *Bacillus amyloliquefaciens* culture filtrates.[35] Anwar et al.[36] found this chemical in the extract from diverse bacterial strains isolated from soil around plant roots. They also showed its antifungal activity against plant pathogenic fungi. The Quinones family includes 2,5-Cyclohexadiene-1,4-dione, 2,5-dihydroxy-3-methoxy-6-methyl- is a natural product, usually found in the plant extract, and it had antimicrobial, antifungal activity, antioxidant, antitumor and anticancer properties.[38,39] The compounds found in the *K. flava* extract potentially had the ability to reduce silver ions to silver nanoparticles, due to their presence within the structural framework of bacterial proteins and enzymes. Additionally, these compounds may also contribute to the stabilization of the nanoparticles by capping them.

Biosynthesis of silver nanoparticles

In this study, silver nanoparticles (AgNPs) were prepared using the culture supernatant of *K. flava*. The color of this supernatant was transformed from yellow to dark brown after adding silver nitrate at a concentration of 1 mM Fig. 4. This alteration occurred over a period of 5 to 7 days, at a temperature of 37°C, and continuous agitation at a rate of 180 rpm in a shaking incubator, ensuring isolation from light sources. This observed change in color serves as an initial indication of the potential formation of silver nanoparticles.[11]

Characterization of biosynthesized silver nanoparticles

UV-Visible spectroscopy

The UV-Visible spectrophotometer detected silver nanoparticles at wavelength 280–800 nm. The single strong peak was at 390 nm as shown in Fig. 5 due to the formation of Surface Plasmon Resonance (SPR) which occurs on metal surfaces when free electrons

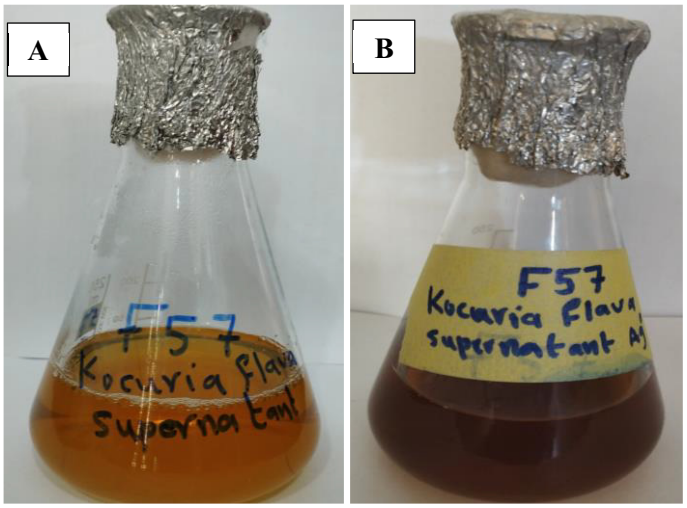


Fig. 4. *K. flava* culture supernatant. A- Before adding $AgNO_3$, B- After adding $AgNO_3$ and biosynthesized AgNPs.

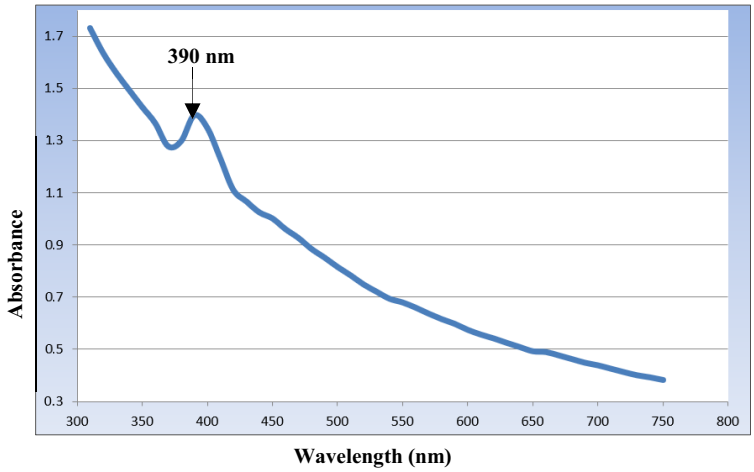


Fig. 5. UV-Visible spectrum of AgNPs biosynthesized by extracellular metabolites of marine *Kocuria flava*, the strong peak of Surface Plasmon Resonance (SPR) was at 390 nm.

within nanoparticles move together in response to incident light. The solution for turning yellow to brown may be due to this feature. This may be due to secondary metabolites present in the filtrate of the bacterial culture, which are responsible for the reduction of metal ions.[40] Many studies have demonstrated the utilization of the UV-visible light spectrum for the detection of metal nanoparticles, such as silver nanoparticles. These studies had focused on identifying the wavelength at which the highest absorption peak occurs. Some studies reported an absorption peak at a wavelength range of 380–395 nm for the highest absorption peak.[41,42] While, several other studies have suggested that the highest absorption peak typically falls within the wavelength range of 400–470 nm.[43–46] The non-appearance of the absorption peak at a certain wavelength may be attributed to variations in the particle size inside the solution and the characteristics of their surface.

Fourier transform infrared spectroscopy (FTIR)

FTIR Spectroscopy was used to identify the functional groups in the biomolecules present in the bacterial culture supernatant of *K. flava*, which are responsible for the bio-reduction of silver ions into silver nanoparticles, as many bands appeared in both the bacterial filtrate and the silver nanoparticle sample as shown in Fig. 6, A&B, and it was compared to the table of functional groups and standard frequency values for the IR spectrum. Several bands appeared in the bacterial filtrate in the range 1000–3500 cm^{-1} indicating to the active groups O-H for phenol, alcohol and carboxylic acids, N-H and C-N groups for aliphatic and aromatic amino acids, C-H and C=C

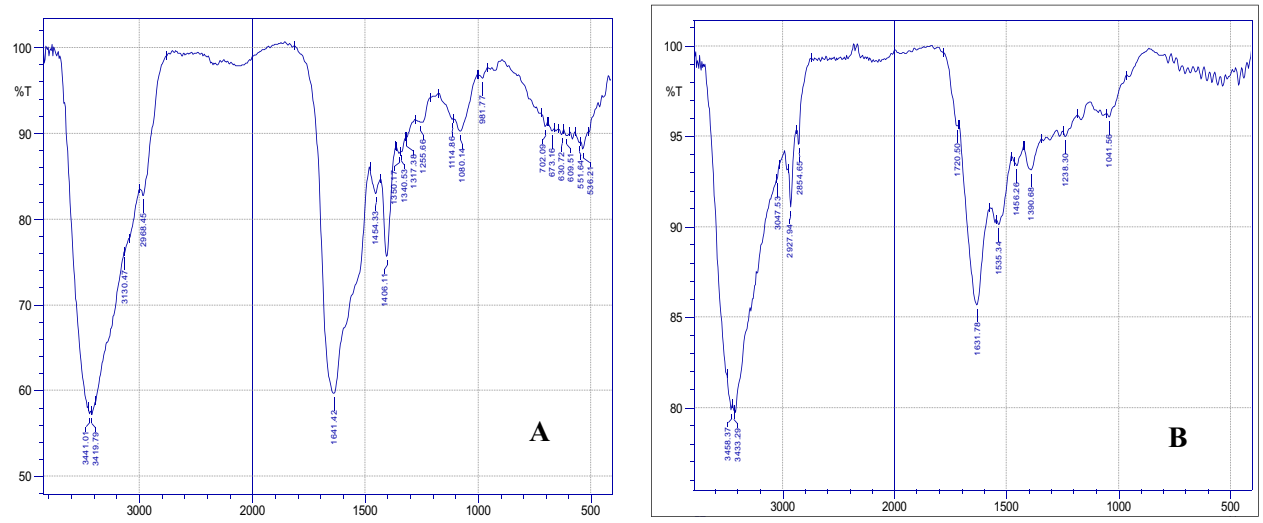


Fig. 6. FTIR spectrum of: A- culture supernatant of *K. flava*, B- AgNPs sample.

groups for alkanes and alkenes, and S = O group for sulfonate. So, the presence of these functional groups in the culture filtrate of *K. flava* implies presence of proteins, enzymes, and some organic compounds may be reduced silver ions to the nano-silver and capping it.

The FTIR spectrum showed a considerable shift and disappearance of some bands in AgNPs sample compared to the bacterial culture filtrate; these indicate to the change in secondary structure of protein after reduction of Ag ions to AgNPs due to interaction between proteins and silver nanoparticles.[43] Furthermore, the identification of active groups of amino acids, sulfonate, and some organic compounds such as alkanes and alkenes suggest the existence of proteins that play roles in the capping of AgNPs and enhancing their stability. These results exhibited a resemblance to the outcomes reported by Khalil et al.,[10,11] and Shareef et al.[46]

X-ray diffraction (XRD)

The XRD results indicate that the diffraction pattern aligns with the Joint Committee on Powder Diffraction Standards (JCPDS) No. 84-0713 and 04-0783 standard pattern for silver nanoparticles. Eight distinct peaks were observable at 2Θ ranged between 27°–80°, specifically at 27.81°, 32.23°, 46.20°, 54.8°, 57.45°, 67.31°, 74.31°, and 76.72° are associated with reflections occurring at levels 111, 200, 220, 311, 222, 400, 331, and 410 as shown in Fig. 7, all reflections were associated with pure silver nanoparticles, with the face-centered cubic planes (FCC). The intensity of the peaks reflects a high degree of stability and crystallization of the nanoparticles, due to presence of capping agents (enzymes), and the broad peaks indicate that the size of the particles was very small.[47] The average crystalline size of the silver nanoparticles according to the Debye-Sherrer equation was about 22.60 nm, furthermore, presence of additional peaks at 2Θ may be indicated to organic substances in the bacterial filtrate that reduced and stabilized silver nanoparticles. The current results were consistent with many previous studies.[45,46]

Determination of size and shape of silver nanoparticles

The physical appearance and compositional features of the silver nanoparticles were determined by FESEM and EDX analysis. The silver nanoparticles exhibited a spherical morphology, with a size ranging from 29.03 to 49.13 nm Fig. 8, thereby confirming their classification within the nanoscale regime. The verification of the existence and purity of silver was established by EDX analysis, the examination revealed the presence of a peak in the 3 kiloelectron volt (KeV) Fig. 9, which is characteristic of the element silver due to SPR. The weight percentage (wt.%) of silver was determined to be 72.7%, indicating the sample exhibits a high level of silver purity. The presence of carbon and oxygen, their occurrence was observed at very low weight percentages of 16.9% and 3.3% respectively. It is plausible that these impurities originated from the proteins found in the bacterial culture filtrate, perhaps forming a connection with the silver via the amine or thiol groups present in those proteins. Regarding the existence of elemental substances, gold and chlorine are present as contaminants in the sample owing to their use in

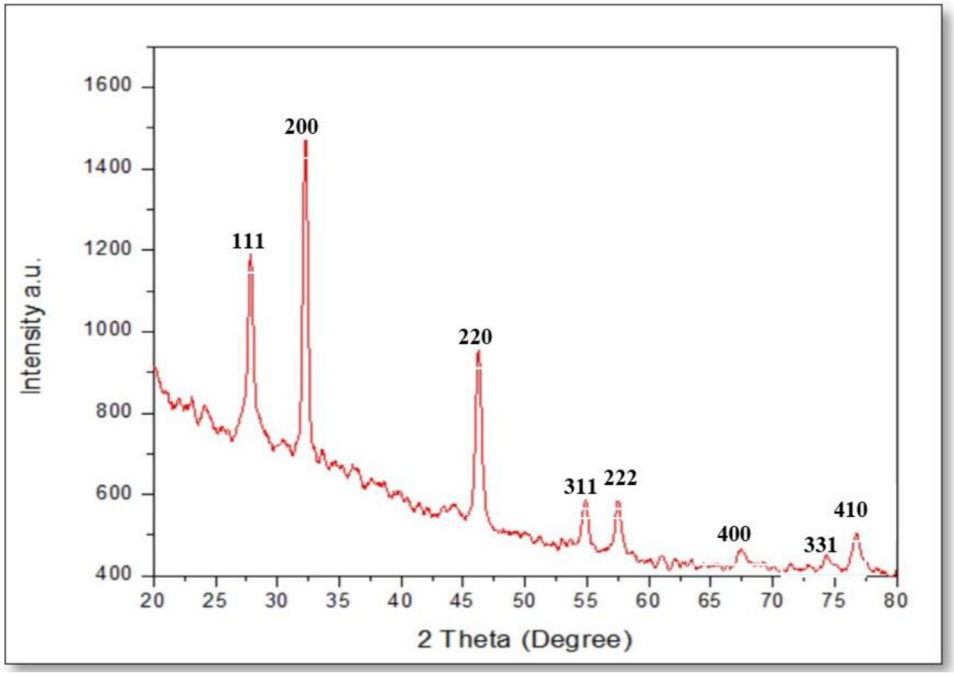


Fig. 7. XRD pattern of AgNPs synthesized by culture supernatant of *Kocuria flava*.

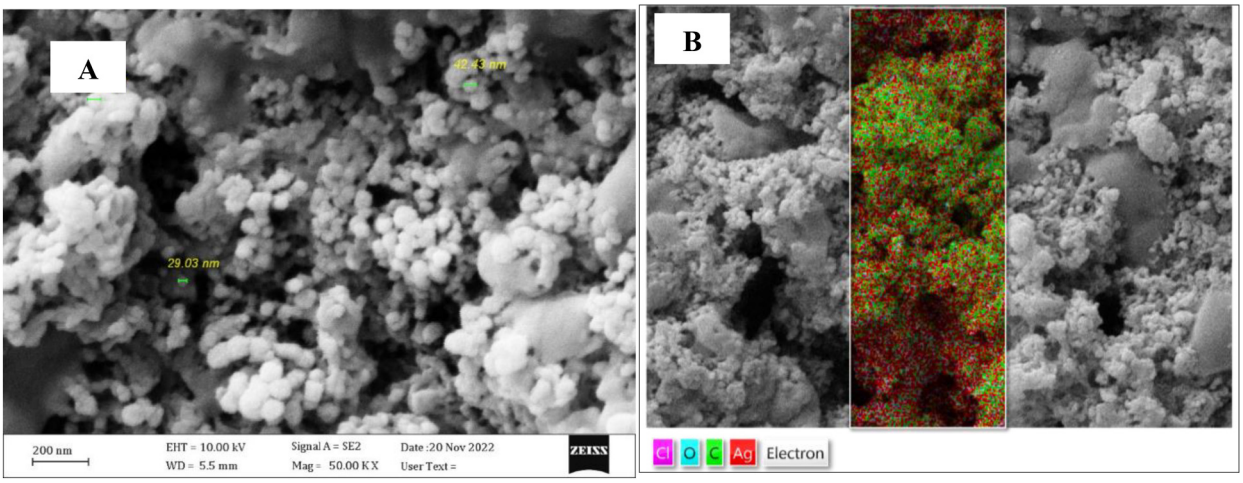


Fig. 8. FESEM image of biosynthesized AgNPs by extracellular metabolites of *K. flava*. A- particle size, B- Mapping image.

the process of loading and preparing the sample for analysis using SEM. The size and shape, as well as the chemical composition of the nanoparticles acquired in the present study, align with the description range seen in previous studies.[10–12,46]

Antimicrobial activity of biosynthesized silver nanoparticles

The present study investigates the biological efficacy of biogenic silver nanoparticles, which were synthesized by using *K. flava* culture supernatant. The effectiveness of these nanoparticles was tested against five MDR pathogenic bacterial strains, including *K. pneumoniae, P. aeruginosa*, and *S. haemolyticus*, as well as two isolates of *E. coli* (1&2). Statistical analysis showed that the isolates *K. pneumoniae* and *S. haemolyticus* were most resistant to silver nanoparticles, followed by *P. aeruginosa*; conversely, *E. coli* 2 was most sensitive to nanoparticle efficacy. The concentration of 1000 μg/ml. shown the highest efficacy, followed by the concentration of 500 μg/ml Table 4. This implies that the efficacy of silver nanoparticles exhibits a positive correlation

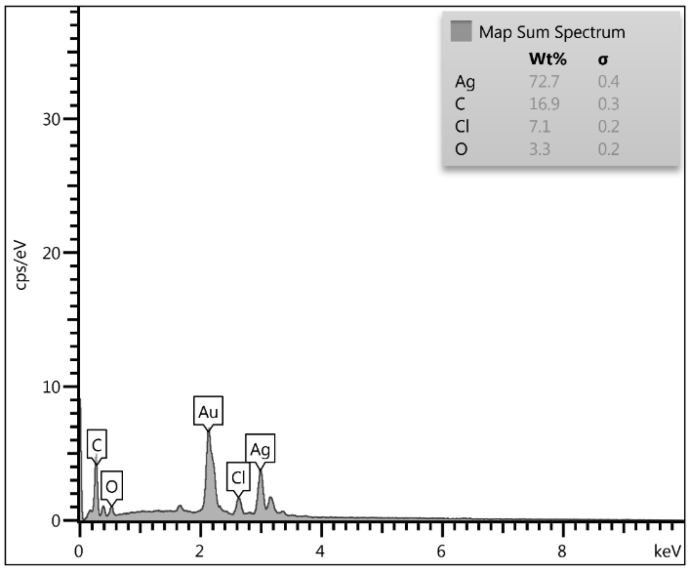


Fig. 9. EDX spectroscopy image of the biosynthesized AgNPs by extracellular metabolites of *K. flava*.

Table 4. Inhibition zone diameter (mm) due to antimicrobial activity of biogenic silver nanoparticles synthesized by *K. flava* culture supernatant.

Bacterial isolates	Concentrations of biogenic AgNPs. ($\mu g/l$)				Average
	1000	500	250	125	
K. pneumoniae	14 ± 0.23	12 ± 0.29	11 ± 0.15	11 ± 0.21	12.00 ± 1.4^{a}
P. aeruginosa	13 ± 0.21	13 ± 0.32	12 ± 0.29	12 ± 0.35	12.50 ± 0.6^{ab}
S. haemolyticus	14 ± 0.12	14 ± 0.06	13 ± 0.12	12 ± 0.40	12.25 ± 0.9^{a}
E. coli 1	15 ± 0.23	14 ± 0.10	12 ± 0.25	11 ± 0.06	13.00 ± 1.8^{bc}
E. coli 2	15 ± 0.06	14 ± 0.15	12 ± 0.12	11 ± 0.32	13.00 ± 1.8^{c}
Average ($p \leq 0.05$)	14.2 ± 1.1^{a}	13.2 ± 1.1^{b}	11.6 ± 0.9^{c}	11.2 ± 0.9^{c}	12.50 ± 1.5

with higher concentrations, and these results closely align with previous studies.[11,46,48]

The development of mechanisms of antibiotic resistance in pathogenic bacteria poses a significant global concern and represents a grave threat to human health. Consequently, researchers are exploring alternative strategies to overcome resistance mechanisms exhibited by pathogenic bacteria. One such alternative being investigated is the utilization of silver nanoparticles, owing to their diverse applications across various domains, including the medical sector.[49] The present investigation has demonstrated the capacity of silver nanoparticles to inhibit the growth of pathogenic bacterial strains that exhibit resistance to several antibiotics. It is worth noting that our understanding of the underlying mechanisms by which nanoparticles exert their effects on living cells remains limited. Nevertheless, other potential processes have been postulated about the impact of silver nanoparticles on bacterial cells. The specific effect of these nanoparticles on bacterial cells is contingent upon factors such as the surface charge, as well as the size and shape of the nanoparticles. Silver nanoparticles' positive charge attracts the negative charge on the bacterial cell wall, outer envelope, and plasma membrane such as lipopolysaccharides and thiol groups in the outer shell components, and the amine groups in the amino acids that make up the peptide chains of peptidoglycan in the cell wall, or the amino acids in the plasma membrane, Nanoparticles have a higher surface area than their size, which improves contact with bacterial cells. This interaction alters plasma membrane permeability, and the bacterial cell's envelope breaks, releasing its contents and killing it.[50] Nanoparticles' small size and high kinetic energy allow them to enter bacterial cells and alter them. This effect increases with smaller nanoparticles. Nanoparticle penetration into cells has several impacts. It produces and accumulates reactive oxygen species (ROS), causing intracellular oxidative stress. These chemicals disturb the entire cellular system and cause apoptosis. It also inhibits ATP generation and respiratory chain enzyme activity by attaching to their active sites. It also inhibits DNA replication, mRNA transcription, as well as their interaction with ribosomes, so, the synthesis of

Table 5. The MIC, and FICI values of ciprofloxacin alone, biogenic silver nanoparticles alone, and their combination against MDR pathogenic bacteria.

Bacterial isolates	MIC values (μg/ml)				FICI values	
	CIP alone	AgNPs alone	CIP after combination with AgNPs	AgNPs after combination with CIP		
K. pneumoniae	64.0	15.63	8.0	7.81	0.6	P.S.
P. aeruginosa	64.0	7.81	4.0	3.90	0.5	S.
S. haemolyticus	128.0	31.25	8.0	15.63	0.5	S.
E. coli 1	0.50	15.63	0.12	7.81	0.7	P.S.
E. coli 2	0.50	31.25	0.03	15.63	0.5	S.

CIP: Ciprofloxacin, AgNPs: Biogenic silver nanoparticles, P.S.: Partial Synergism, S.: Synergism.

cellular proteins is impeded. It interacts with phosphate and sulfur groups in DNA, RNA, and proteins leading to their degradation. These several impacts kill the bacterial cell.[42,50] Singh et al.,[51] has been observed that nanoparticles exhibiting a triangular or hexagonal shape possess a higher antibacterial efficacy compared to nanoparticles with a spherical shape. Mohammad and Al-Jubouri[52] found the silver nanoparticles biosynthesized by *Corynebacterium glutamicum* were more effective against MDR bacteria than those biosynthesized by plant extract.

Generally, bacteria cannot build resistance to silver nanoparticles' varied effects. Silver nanoparticles assault several exterior and internal targets in the bacterial cell. Most antibiotics attack a single target in bacterial cell. Thus, bacteria can develop antibiotic resistance by producing enzymes that break down the antibiotic's active components, shielding or obstructing the target, or preventing the antibiotic from entering the cell and eliminating the antibiotic molecules which succeeded in entering the bacterial cell and flowing out of the cell by efflux pumps, so the sensitivity of pathogenic bacteria to the effectiveness of silver nanoparticles makes them one of the suitable alternatives to overcome those pathogenic bacteria that have developed resistance to antibiotics.[11]

Synergism of biosynthesized silver nanoparticles with ciprofloxacin by micro-dilution method

The MIC of ciprofloxacin and biogenic silver nanoparticles (AgNPs) and mixture between were tested by used microdilution (Checkerboard) method, to determine if the AgNPs may be enhancing this antibiotic efficiency against MDR pathogenic bacteria. The MIC values of silver nanoparticles were ranged from 7.81 to 31.25 μg/ml. All five isolates were ciprofloxacin-resistant when MIC values were compared to values in the CLSI (2022). The results of mixing biogenic silver nanoparticles and ciprofloxacin, showed the silver nanoparticles increased the efficiency of this antibiotic by 2 to 4-fold, according to the MIC values. The FICI values indicated a synergistic interaction between silver nanoparticles and the ciprofloxacin, resulting in a notable increase in efficiency against *P. aeruginosa*, *S. haemolyticus*, and *E. coli* (2) isolates (FICI $\leq$ 0.5). While the effect of silver nanoparticles was partial synergy for the effectiveness of this antibiotic for *K. pneumoniae* and *E. coli* (1) isolates, and the FICI values were 0.6 and 0.7 respectively Table 5. Generally, silver nanoparticles boost the antibiotic effectiveness against MDR pathogens, and the isolates *E. coli* (1&2) became sensitive to this antibiotic after mixing with silver nanoparticles, the MIC values decrease from 0.5 μg/ml for *E. coli* (1) and *E. coli* (2) isolates to 0.12 μg/ml and 0.03 μg/ml respectively. The MIC values were found to be rather low, closely resembling the obtained values of previous studies.[10,11]

Ciprofloxacin is a broad-spectrum fluoroquinolone antibiotic. Gram-positive and Gram-negative bacterial infections are treated with this drug. It must also enter the bacterial cell to affect the DNA molecule. It binds with A subunit of DNA gyrase, which unwinds the DNA helix for replication and preventing DNA replication and cell division. It also inhibits Topoisomerase IV, which cleaves and eliminates the DNA that results from replication and dissociation from the template strand.[53]

Silver nanoparticles bind with functional groups of ciprofloxacin like carbonyl (-C=O), carboxyl (-C(=O)-OH), and fluorine to create a stable complex with the antibiotic. Bayroodi and Jalal[24] found synergistic effect between zinc oxide nanoparticles and three antibiotics, including ciprofloxacin against *P. aeruginosa*, and they indicated the possibility of zinc elements in zinc oxide nanoparticles may interact with ciprofloxacin's active groups, suggesting that they transport the antibiotic, this synergetic effect due to zinc oxide nanoparticles disrupting the cell membrane and expelling cellular contents, the altered permeability of the plasma membrane allows antibiotic molecules to bypass efflux pumps and inter into bacterial cell. In addition to the silver nanoparticles' extra effects, by increasing oxidative stress, inhibiting enzymes, DNA damage and other effects which accelerate cell death. Tharwat et al.[8] found

that silver nanoparticles and ciprofloxacin synergistically inhibit *P. aeruginosa*, the combination use of both drugs increased efficiency by two to thrice. Hussein-Al-Ali et al.[54] discovered that silver nanoparticles form a stable combination with ciprofloxacin's hydroxyl groups, and this combination helps deliver ciprofloxacin to microorganisms. Khalil et al.[10,11] found that silver nanoparticles and antibiotics synergize, they reported a reduction in the MIC values for both silver nanoparticles and antibiotics following their combination due to binding between silver nanoparticles and carboxyl and hydroxyl functional groups of antibiotic piperacillin-tazobactam.

Conclusion

High salinity concentrations characterize Iraqi marine waters, tend to be alkaline, and have a high content of total dissolved salts (TDS). They are a good source of various bacterial species, including *K. flava*. The extracellular metabolites of these marine bacteria contain many chemical compounds that contribute to reducing silver ions in silver nitrate and the biosynthesis of silver nanoparticles in an eco-friendly, easy, and inexpensive process. The UV-visible spectra, FTIR spectra, XRD, FESEM, and EDX were useful to confirm the success of the biosynthesis of silver nanoparticles and to know their morphological characteristics and chemical composition. These biosynthesized silver nanoparticles have antimicrobial activity against MDR pathogenic bacteria. These silver nanoparticles effectively contributed to enhancing the antibacterial effectiveness of ciprofloxacin against MDR bacteria, which were resistant to it. There was a synergistic effect between silver nanoparticles and ciprofloxacin against some pathogenic isolates, so it is possible to use silver nanoparticles to enhance the effectiveness of antibiotics against MDR pathogens after testing their cytotoxicity.

Acknowledgment

The authors would like to express their sincere appreciation to the Department of Biology—College of Education for Pure Sciences—University of Basrah for their invaluable support in facilitating the completion of this research project.

Authors' declaration

- Conflicts of Interest: None.
- We hereby confirm that all the Figures and Tables in the manuscript are ours. Furthermore, any Figures and images that are not ours have been included with the necessary permission for republication, which is attached to the manuscript.
- No animal studies are present in the manuscript.
- No human studies are present in the manuscript.
- Ethical Clearance: The project was approved by the local ethical committee at the University of Basrah—College of Education for Pure Science.

Authors' contribution statement

F.J. and A.A. designed and planned this study, performed the experiments, analyzed the data, finding results, and wrote the paper.

References

1. Adebayo-Tayo BC, Ekundayo-Obaba O, Falodun OI. Antimicrobial potential of bioactive metabolites and silver nanoparticles from bacillus spp. and of some antibiotics against multidrug-resistant salmonella spp. Turkish J Pharm Sci. 2020;17(5):511–522. https://doi.org/10.4274/tjps.galenos.2019.46548.
2. Catalano A, Iacopetta D, Ceramella J, Scumaci D, Giuzio F, Saturnino C, *et al.* Multidrug resistance (MDR): A widespread phenomenon in pharmacological therapies. Molecules. 2022;27(3):616–634. https://doi.org/10.3390/molecules27030616.
3. Singh AA, Singh AK, Nerurkar A. Bacteria associated with marine macroorganisms as potential source of quorum-sensing antagonists. J Basic Microbiol. 2020;60(9):799–808. https://doi.org/10.1002/jobm.202000231.
4. Gahlawat G, Choudhury AR. A review on the biosynthesis of metal and metal salt nanoparticles by microbes. RSC Adv. 2019;9(23):12944–12967. https://doi.org/10.1039/c8ra10483b.
5. Abbas AZ, Abdulrahman RB, Mustafa TA. Preparation and characterization of silver nanoparticles and its medical application against pathogenic bacteria. Baghdad Sci J. 2024;21(1):204–216. https://doi.org/10.21123/bsj.2023.7763.
6. Li P, Li J, Wu C, Wu Q, Li J. Synergistic antibacterial effects of β-lactam antibiotic combined with silver nanoparticles. Nanotechnology. 2005;16:1912–1917. https://doi.org/10.1088/0957-4484/16/9/082.
7. Singh R, Wagh P, Wadhwani S, Gaidhani S, Kumbhar A, Bellare J, *et al.* Synthesis, optimization, and characterization of silver nanoparticles from *Acinetobacter calcoaceticus* and their enhanced antibacterial activity when combined with antibiotics. Int J Nanomedicine. 2013;8:4277–90. https://doi.org/10.2147/IJN.S48913.
8. Tharwat NA, Saleh NM, Hamouda RE, El Shreif RH, Elnagdy SM, Mohamed G. Combination of ciprofloxacin and silver nanoparticles for treatment of multi-drug resistant *Pseudomonas aeruginosa* in Egypt. Al-Azhar J Pharm Sci. 2019;59(1):107–122. https://doi.org/10.21608/ajps.2019.64110.
9. Khalil MA, El Maghraby GM, Sonbol FI, Allam NG, Ateya PS, Ali SS. Enhanced efficacy of some antibiotics in presence of silver nanoparticles against multidrug resistant *Pseudomonas aeruginosa* recovered from burn wound infections. Front

Microbiol. 2021;12:648560. https://doi.org/10.3389/fmicb.2021.648560.
10. Khalil MA, El-Shanshoury AERR, Alghamdi MA, Sun J, Ali SS. *Streptomyces catenulae* as a novel marine actinobacterium mediated silver nanoparticles: Characterization, biological activities, and proposed mechanism of antibacterial action. Front Microbiol. 2022;13:833154. https://doi.org/10.3389/fmicb.2022.833154.
11. Khalil MA, El-Shanshoury AER, Alghamdi MA, Alsalmi FA, Mohamed SF, Sun J, *et al.* Biosynthesis of silver nanoparticles by marine actinobacterium *Nocardiopsis dassonvillei* and exploring their therapeutic potentials. Front Microbiol. 2022;12:705673. https://doi.org/10.3389/fmicb.2021.705673.
12. Haji SH, Ali FA, Aka STH. Synergistic antibacterial activity of silver nanoparticles biosynthesized by carbapenem-resistant gram-negative bacilli. Sci Reports. 2022;12(1):15254. https://doi.org/10.1038/s41598-022-19698-0.
13. Hasson SO, Salman SAK, Hassan SF, Abbas SM. Antimicrobial effect of eco-friendly silver nanoparticles synthesis by Iraqi date palm (*Phoenix dactylifera*) on gram-negative biofilm-forming bacteria. Baghdad Sci J. 2021;18(4):1149–1156. https://doi.org/10.21123/bsj.2021.18.4.1149.
14. Syakti AD, Lestari P, Simanora S, Sari LK, Lestari F, Idris F, *et al*. Culturable hydrocarbonoclastic marine bacterial isolates from Indonesian seawater in the lombok strait and Indian ocean. Heliyon. 2019;5(5):e01594. https://doi.org/10.1016/j.heliyon.2019.e01594.
15. Amdadul Huq M, Akter S. Characterization and genome analysis of *Arthrobacter bangladeshi* sp. Nov., applied for the green synthesis of silver nanoparticles and their antibacterial efficacy against drug-resistant human pathogens. Pharmaceutics. 2021; 13(10). https://doi.org/10.3390/pharmaceutics13101691.
16. Prescott H. Laboratory exercises in microbiology. 5th.Ed. McGraw−Hill Companies. New York, USA, 2002;449p.
17. Wilson KH, Blitchington RB, Greene RC. Amplification of bacterial 16S ribosomal DNA with polymerase chain reaction. J Clin Microbiol. 1990;28(9):1942–1946. https://doi.org/10.1128/jcm.28.9.1942-1946.1990.
18. Raji AI, Möller C, Litthauer D, van Heerden E, Piater LA. Bacterial diversity of biofilm samples from deep mines in South Africa. Biokemistri. 2008;20(2):53–62.
19. Tamura K, Stecher G, Kumar S. MEGA11: Molecular evolutionary genetics analysis version 11. Mol Biol Evol. 2021;38(7):3022-3027. https://doi.org/10.1093/molbev/msab120.
20. Naveed M, Ishfaq H, Rehman SU, Javed A, Waseem M, Makhdoom SI, *et al*. GC–MS profiling of *Bacillus* spp. metabolites with an in vitro biological activity assessment and computational analysis of their impact on epithelial glioblastoma cancer genes. Front Chem. 2023;11:1–14. https://doi.org/10.3389/fchem.2023.1287599.
21. Goel N, Ahmad R, Singh R, Sood S, Khare SK. Biologically synthesized silver nanoparticles by *Streptomyces* sp. EMB24 extracts used against the drug-resistant bacteria. Bioresour Technol Rep. 2021;15(2):100753. https://doi.org/10.1016/j.biteb.2021.100753.
22. Perez C, Pauli M, Bazerque P. An antibiotic assay by the agar well diffusion method. Acta Biol Med Exp. 1990; 15(1):113–115. https://www.researchgate.net/publication/303960600.
23. Bellio P, Fagnani L, Nazzicone L, Celenza G. New and simplified method for drug combination studies by checkerboard assay. MethodsX. 2021;8:101543. https://doi.org/10.1016/j.mex.2021.101543.
24. Bayroodi E, Jalal R. Modulation of antibiotic resistance in *Pseudomonas aeruginosa* by ZnO nanoparticles. Iran J Microbiol. 2016;8(2):85–92..
25. Fadwa AO, Alkoblan DK, Mateen A, Albarag AM. Synergistic effects of zinc oxide nanoparticles and various antibiotics combination against *Pseudomonas aeruginosa* clinically isolated bacterial strains. Saudi J Biol Sci. 2021;28(1):928–935. https://doi.org/10.1016/j.sjbs.2020.09.064.
26. Omer NH. Water Quality Parameters. In: Summers JK, ed. Water Quality - Science, Assessments and Policy. IntechOpen. 2020. https://doi.org/10.5772/intechopen.89657.
27. Shareef NF, Mahdi MM. Studying of recent environments in Faw, Khor Al-Zubair and Um-Qaser areas, Southwestern Arabian Gulf, Basrah, Iraq. J Basrah Rese ((Sci)). 2015;41(2):1–14.
28. Jaafar RS, Al-Taee A, Al-Kanany FN. Bacterial diversity in different positions in the Iraqi marine area. Baghdad Sci J. 2023;20(1):1–6. https://doi.org/10.21123/bsj.2022.6610.
29. Aertsen A, Meersman F, Hendrick MEG, Vogel RF, Michiels CW. Biotechnology under high pressure: Applications and implications. Trends Biotechnol. 2009;27:434–441. https://doi.org/10.1016/j.tibtech.2009.04.001.
30. Zhou G, Luo X, Tang Y, Zhang L, Yang Q. *Kocuria flava* sp. nov. and *Kocuria turfanensis* sp. nov., airborne actinobacteria isolated from Xinjiang, China. Int J Syst Evol Microbiol. 2008;1:1304–1307. https://doi.org/10.1099/ijs.0.65323-0.
31. Sun W, Liu C, Zhang F, Zhao M, Li Z. Comparative genomics provides insights into the marine adaptation in sponge-derived *Kocuria flava* S43. Front Microbiol. 2018;9:1257–1268. https://doi.org/10.3389/fmicb.2018.01257.
32. Deutsch Y, Samara M, Nasser A, Berman-Frank I, Ezra D. *Kocuria flava*, a Bacterial Endophyte of the Marine Macroalga *Bryopsis plumosa*, Emits 8-Nonenoic Acid Which Inhibits the Aquaculture Pathogen *Saprolegnia parasitica*. Mar Drugs. 2023;21(9):476–488. https://doi.org/10.3390/md21090476.
33. Kiran GS, Priyadharsini S, Sajayan A, Ravindran A, Selvin J. An antibiotic agent pyrrolo[1,2-: A] pyrazine-1,4-dione,hexahydro isolated from a marine bacteria *Bacillus tequilensis* MSI45 effectively controls multi-drug resistant *Staphylococcus aureus*. RSC Adv. 2018;8(32):17837–17846. https://doi.org/10.1039/C8RA00820E.
34. Ser HL, Palanisamy UD, Yin WF, Abd Malek SN, Chan KG, Goh BH, *et al.* Presence of antioxidative agent, Pyrrolo[1,2-a]pyrazine-1,4-dione, hexahydro- in newly isolated *Streptomyces mangrovisoli* sp nov. Front Microbiol. 2015;6:854. https://doi.org/10.3389/fmicb.2015.00854.
35. Raut LS, Rakh RR, Hamde VS. *In vitro* biocontrol scenarios of *Bacillus amyloliquefaciens* subsp. *amyloliquefaciens* strain rls19 in response to *Alternaria macrospora*, an *Alternaria* leaf spot phytopathogen of bt cotton. J Appl Biol Biotechnol. 2021;9(1):75–82. http://dx.doi.org/10.7324/JABB.2021.9110.
36. Anwar S, Mahmood F, Tahir NA, Salih GF. Secondary Compounds Released By Rhizospheric Bacteria Exhibit Fungistatic Effects Against Phytopathogenic Fungus. Iraqi J Agric Sci. 2022;53(5):1174–1183. https://doi.org/10.36103/ijas.v53i5.1631.
37. Manimaran M, Kannabiran K. Marine *Streptomyces* sp. VITMK1 derived Pyrrolo [1, 2-A] Pyrazine-1, 4-Dione, Hexahydro-3-(2-Methylpropyl) and its free radical scavenging activity. Open Bioact Compd J. 2017;5(1):23–30. http://dx.doi.org/10.2174/1874847301705010023.
38. Carcamo-Noriega EN, Sathyamoorthi S, Banerjee S, Gnanamani E, Mendoza-Trujillo M, Mata-Espinosa D, *et al.* 1,4-Benzoquinone antimicrobial agents against *Staphylococcus*

aureus and *Mycobacterium tuberculosis* derived from scorpion venom. Proc Natl Acad Sci U S A. 2019;116(26):12642–12647. https://doi.org/10.1073/pnas.1812334116.

39. da Silva RE, Ribeiro FOS, de Carvalho AMA, Daboit TC, Marinho-Filho JDB, Matos TS, *et al.* Antimicrobial and antibiofilm activity of the benzoquinone oncocalyxone A. Microb Pathog. 2020;149(September):104513. https://doi.org/10.1016/j.micpath.2020.104513.
40. Shanshoury AERE, Sabae SZ, Shouny WAE, Shady AMA, Badr HM. Extracellular biosynthesis of silver nanoparticles using aquatic bacterial isolate and its antibacterial and antioxidant potentials. Egypt J Aquat Biol Fish. 2020; 24(7 Special issue):183–201. http://dx.doi.org/10.21608/EJABF.2020.119399.
41. Al-Hayanni HSA, Alnuaimi MT, Al-Lami RAH, Zaboon SM. Antibacterial effect of silver nanoparticles prepared from *Sophora flavescens* root aqueous extracts against multidrug-resistance *Pseudomonas aeruginosa* and *Staphylococcus aureus*. J Pure Appl Microbiol. 2022;16(4):2880–2890. https://doi.org/10.22207/JPAM.16.4.61.
42. Yassin MT, Mostafa AAF, Al-Askar AA, Al-Otibi FO. Synergistic antibacterial activity of green synthesized silver nanomaterials with colistin antibiotic against multidrug-resistant bacterial pathogens. Crystals. 2022;12(8):1057. https://doi.org/10.3390/cryst12081057.
43. Alsamhary KI. Eco-friendly synthesis of silver nanoparticles by *Bacillus subtilis* and their antibacterial activity. Saudi J Biol Sci. 2020;27(8):2185–2191. https://doi.org/10.1016/j.sjbs.2020.04.026.
44. Naseer QA, Xue X, Wang X, Dang S, Din SU, Kalsoom Jamil J. Synthesis of silver nanoparticles using *Lactobacillus bulgaricus* and assessment of their antibacterial potential. Brazilian J Biol. 2022;82:e232434. https://doi.org/10.1590/1519-6984.232434.
45. Tufail MS, Liaqat I, Andleeb S, Naseem S, Zafar U, Sadiqa A, *et al.* Biogenic synthesis, characterization and antibacterial properties of silver nanoparticles against human pathogens. J Oleo Sci. 2022;71(2):257–265. https://doi.org/10.5650/jos.ess21291.
46. Shareef AA, Farhan FJ, Alriyahee FAA. Green synthesis of silver nanoparticles using aqueous extract of *Typha domingensis* Pers. pollen (qurraid) and evaluate its antibacterial activity. Baghdad Sci J. 2024;21(1):28–40. https://doi.org/10.21123/bsj.2023.7624.
47. Naganthran A, Verasoundarapandian G, Khalid FE, Masarudin MJ, Zulkharnain A, Nawawi NM, *et al.* Synthesis, characterization and biomedical application of silver nanoparticles. Materials (Basel). 2022;15(2):1–43. https://doi.org/10.3390%2Fma15020427.
48. Shareef AA, Hassan ZA, Kadhim MA, Al-Mussawi AA. Antibacterial activity of silver nanoparticles synthesized by aqueous extract of *Carthamus oxycantha* M. Bieb. against antibiotics resistant bacteria. Baghdad Sci J. 2022;19(3):460–468. https://doi.org/10.21123/bsj.2022.19.3.0460.
49. Nile SH, Baskar V, Selvaraj D, Nile A, Xiao J, Kai G. Nanotechnologies in food science: Applications, recent trends, and future perspectives. Nanomicro Lett. 2020;12(1):45–79. https://doi.org/10.1007/s40820-020-0383-9.
50. Qin W, Wang CY, Ma YX, Shen MJ, Li J, Jiao K, *et al.* Microbe-mediated extracellular and intracellular mineralization: environmental, industrial, and biotechnological applications. Adv Mater. 2020;32(22):e1907833. https://doi.org/10.1002/adma.201907833.
51. Singh S, Bharti A, Meena VK. Green synthesis of multi-shaped silver nanoparticles: optical, morphological and antibacterial properties. J Mater Sci: Mater Electron. 2015;26(6):3638–3648. http://dx.doi.org/10.1007/s10854-015-2881-y.
52. Mohammad D, Al-Jubouri SHK. Comparative antimicrobial activity of silver nanoparticles synthesized by *Corynebacterium glutamicum* and plant extracts. Baghdad Sci J. 2019;16(3):689–696. https://doi.org/10.21123/bsj.2019.16.3(Suppl.)0689.
53. Sharma PC, Jain A, Jain S, Pahwa R, Yar MS. Ciprofloxacin: Review on developments in synthetic, analytical, and medicinal aspects. J Enzyme Inhib Med Chem. 2010; 25(4):577–589. https://doi.org/10.3109/14756360903373350.
54. Hussein-Al-Ali SH, Abudoleh SM, Abualassal QIA, Abudayeh Z, Aldalahmah Y, Hussein MZ. Preparation and characterisation of ciprofloxacin-loaded silver nanoparticles for drug delivery. IET Nanobiotechnol. 2022;16(3):92–101. https://doi.org/10.1049/nbt2.12081.

التصنيع الحيوي لدقائق الفضة النانوية باستخدام الأيوض الخارج خلوية للبكتيريا البحرية *Kocuria flava* واختبار دورها في تعزيز الفعّالية الضد ميكروبية للسيبروفلوكساسين

فاضل جبار فرحان، علي عبود شريف

قسم علوم الحياة، كلية التربية للعلوم الصرفة، جامعة البصرة، البصرة، العراق.

الخلاصة

تهدف الدراسة الحالية إلى تصنيع دقائق الفضة النانوية (AgNPs) حيوياً باستخدام الأيوض الخارج خلوية للبكتيريا البحرية *Kocuria flava* (F57)، وأستخدامها لتعزيز فعّالية المضاد الحيوي السيبروفلوكساسين تجاه البكتيريا المرضية ذات المقاومة المتعددة للمضادات الحيوية (MDR). جُمعت عيّنات المياه البحرية من المياه البحرية العراقية خلال شهر كانون الثاني/2022. تم تشخيص العزلةF57 من خلال الصفات المجهرية، وبعض الاختبارات الكيموحيوية، والتشخيص الجزيئي بتضخيم الجين *16S rDNA*، وظهر من خلال رصف تسلسلات القواعد النايتروجينية للجين *16S rDNA* مع تلك العائدة للسلالات المسجّلة في بنك الجينات NCBI، وشجرة النشوء والتطور، وجود تطابق نسبته 99.93% مع السلالة *K. flava* AUMC B-459. أظهرت نتائج قياس الطيف الكتلي GC/MS لمستخلص العزلة F57 وجود ثلاثين مركباً. أُستخدمت الأيوض الخارج خلوية للعزلة F57 لتصنيع دقائق الفضة النانوية، وتم التأكد من نجاح عملية تصنيع الحيوي عن طريق التحليل الطيفي للضوء المرئي- الأشعة فوق البنفسجية وطيف الأشعة تحت الحمراء وحيود الأشعة السينية والمجهر الإلكتروني الماسح وطاقة تشتت طاقة الأشعة السينية. أظهرت دقائق الفضة النانوية فعّالية تجاه خمس عزلات من البكتيريا المرضية ذات المقاومة المتعددة للمضادات الحيوية وهي كلٌ من:*Klebsiella pneumoniae*، *Pseudomonas aeruginosa*، *Staphylococcus haemolyticus*، وعزلتان من البكتيريا *Escherichia coli* (1&2)، تم تحديد التركيز المثبّط الأدنى لدقائق الفضة النانوية والمضاد الحيوي Ciprofloxacin ومزيجهما معاً ضد العزلات البكتيرية المرضية أعلاه، وكانت العزلة *P. aeruginosa* هي الأكثر حساسية لدقائق الفضة النانوية، إذ كان التركيز المثبطّ الأدنى تجاهها 7.81 مايكروغرام/مل، وكانت جميع العزلات البكتيّرية المرضية مقاومة للمضاد الحيوي Ciprofloxacin، وأظهرت نتائج مزج المضاد الحيوي Ciprofloxacin مع دقائق الفضة النانوية وجود تأثير تآزري تجاه العزلات المرضية *P. aeruginosa* و *S. haemolyticus* و(2) *E. coli* ، وأصبحت العزلتين (1&2) *E. coli* حساسة لهذا المضاد الحيوي بعد عملية المزج. لذا فإن دقائق الفضة النانوية المخلّقة حيوياً بإستخدام الأيوض الخارج خلوية للبكتيريا البحرية (F57) *K. flava* ذات خصائص مضادة للبكتيريا المرضية، وقد أسهمت في تعزيز فعّالية المضاد الحيوي Ciprofloxacin.

الكلمات المفتاحية: دقائق الفضة النانوية، تعزيز نشاط المضاد الحيوي، Ciprofloxacin، *Kocuria flava*، البكتيريا المقاومة للمضادات الحيوية MDR.